

METOP SECOND GENERATION SCATTEROMETER MISSION

**Franco Fois , Chung-Chi Lin, Hubert Barré, Maurizio Betto, Marc Loiselet
and Graeme Mason**

European Space Agency, Keplerlaan 1, 2200 AG Noordwijk ZH, The Netherlands

Abstract

ESA is currently running two parallel, competitive phase A/B1 studies for MetOp Second Generation (MetOp-SG). MetOp-SG is the space segment of EUMETSAT Polar System (EPS-SG) consisting of the satellites and instruments. The Phase A/B1 studies will be completed at the end of 2012. The final implementation phases (B2/C/D) are planned to start 2013.

ESA is responsible for instrument design of five missions, namely Microwave Sounding Mission (MWS), Scatterometer mission (SCA), Radio Occultation mission (RO), Microwave Imaging mission (MWI) and Multi-viewing, multi-channel, multi-polarisation imaging mission (3MI).

The Scatterometer (SCA) is one of the high-priority payload instruments to provide vector surface wind observations over the ocean, which constitutes an important input to numerical weather prediction (NWP) as well as provides valuable information for tracking of extreme weather events. The SCA shall offer observations with higher spatial resolution than those provided by ASCAT on board MetOp, currently operating at C-band and with VV-polarization. Furthermore, the addition of VH polarization will significantly extend the upper dynamic range of the wind measurements (≤ 40 m/s) and improve the quality of soil moisture product over land.

INTRODUCTION

The Scatterometer (SCA) is one of the high priority payload instruments to provide vector surface wind observations over ocean, which constitute an important input to the NWP as well as valuable information for tracking of extreme weather events. The secondary products derived from the scatterometer data are:

- Land surface soil moisture
- Leaf area index
- Snow water equivalent
- Snow cover
- Sea-ice type
- Sea-ice extent.

The EPS-SG SCA shall offer observations with higher spatial resolution and radiometric stability than those provided by ASCAT on board MetOp. Furthermore, addition of VH polarization on the mid beams will extend the upper dynamic range of the wind measurements (≤ 40 m/s) and improve the quality of soil moisture product over land.

TECHNICAL REQUIREMENTS

The SCA payload is a real-aperture, pulsed imaging radar with six fixed fan beam-antennas. In this configuration, the principal elevation planes of the SCA antenna beams are oriented at 45° (Fore-left), 90° (Mid-left), 135° (Aft-left), 225° (Aft-right), 270° (Mid-right) and 315° (Fore-right) with respect to the flight direction, similar to MetOp's ASCAT as shown in Figure 1. Each of the SCA beams shall acquire a continuous image of the normalised (per-unit-surface) radar backscatter coefficient of the ocean surface, called σ^0 over a swath. Both sides of the sub-satellite track are imaged each with three azimuth views, with an unavoidable observation gap below the satellite. A large number of independent looks are summed in range and azimuth (multi-looking), for each azimuth view, in order to achieve the specified radiometric resolution of the σ^0 estimate on each measurement pixel. The

three σ^0 measurements (σ^0 -triplet) are uniquely related to the 10-m vector wind through the Geophysical Model Function (GMF) [1]. The wind inversion is based on a search for minimum distances between the measured σ^0 -triplet and all the backscatterer model solutions lying on the GMF surface, taking into account instrumental and geophysical noise sources [2]. Due to measurement noise, multiple solutions are usually found (wind ambiguities), which have to be filtered out using the background wind information provided by a NWP model (ambiguity removal).

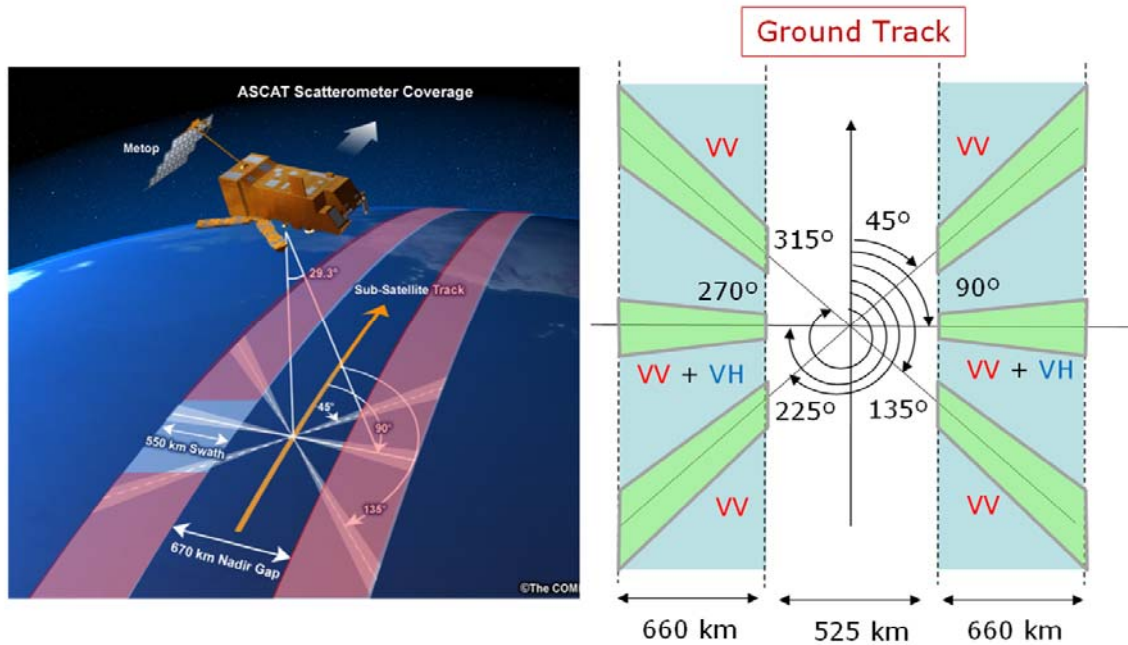


Figure 1: ASCAT measurement geometry (left) versus SCA measurement geometry (right)

As compared to ASCAT, SCA shall have a smaller nadir gap by reducing the minimum incidence angle from 25° (ASCAT) to 20°. The main technical requirements of SCA are reported in Table 1 and compared to the ones of ASCAT. The major improvements to be brought by SCA with respect to ASCAT are the spatial resolution of 25 km × 25 km, the radiometric stability of ≤ 0.1 dB and the addition of VH polarization measurements on mid beams.

Parameter	ASCAT	MetOp-SG SCA
Frequency	5.3 GHz	
Polarisation	VV for all beams	VV for all beams + VH for Mid-beams
Azimuth views	45°, 90° and 135° w.r.t. satellite track	
Min. incidence	25°	20°
Horizontal resolution	Nom: (50 km) ² High res.: (25 - 35 km) ²	Nom: (25 km) ² High res.: (17 - 22 km) ²
Horizontal sampling	Nom: (25 km) ² High res.: (12.5 km) ²	Nom: (12.5 km) ² High res.: (6.25 km) ²
Radiometric resolution	≤ 3 % for $\theta_i \leq 25^\circ$ at 4 m/s cross-wind (VV) (0.175 $\times\theta_i - 1.375$) % for $\theta_i > 25^\circ$ at 4 m/s cross-wind (VV) ≤ 3 % at 25 m/s up-wind	
Radiometric Stability	≤ 0.2 dB	≤ 0.1 dB
Coverage	97 % in 48 hrs.	99 % in 48 hrs.

Table 1: main technical requirements of SCA versus ASCAT

IINSTRUMENT DESIGN

The SCA instrument has 6 antennas, 3 on both sides of the satellite ground-track. All antennas emit in vertical polarization. The 4 side antennas receive only vertically polarized signals, whereas the 2 mid antennas receive both V and H-polarized signals. For the mid antennas, two different concepts are under investigation: simultaneous / non- simultaneous reception of V and H-pol signals. The antennas consist of slotted waveguide arrays, connected through waveguides to the beam-switching matrix. For the Fore-/Aft-antenna assemblies, rotating RF-joints are required for enabling deployment.

The SCA antennas are considered a key component of the instrument, as they have direct impact on performance figures like e.g. radiometric stability. Their stability is therefore considered of utmost importance. The design of the SCA antennas is based on a aluminium support structure and RF elements are also made of aluminium.

A high level SCA-instrument block diagram is depicted in Figure 2. The baseband radar pulse is stored in the digital memory read-out and followed by the digital-to-analogue converter (DAC). The analogue pulse is then up-converted to the carrier frequency by a quadrature mixer. The HPA is driven by a high voltage electronics power conditioner (EPC). The HPA feeds the six antennas sequentially through the beam-switching matrix. The receive signal is amplified by the low noise amplifier (LNA) and down-converted to the in-phase (I) and quadrature phase (Q) baseband signals. The digitized I and Q baseband signals are down-linked and further processed on ground.

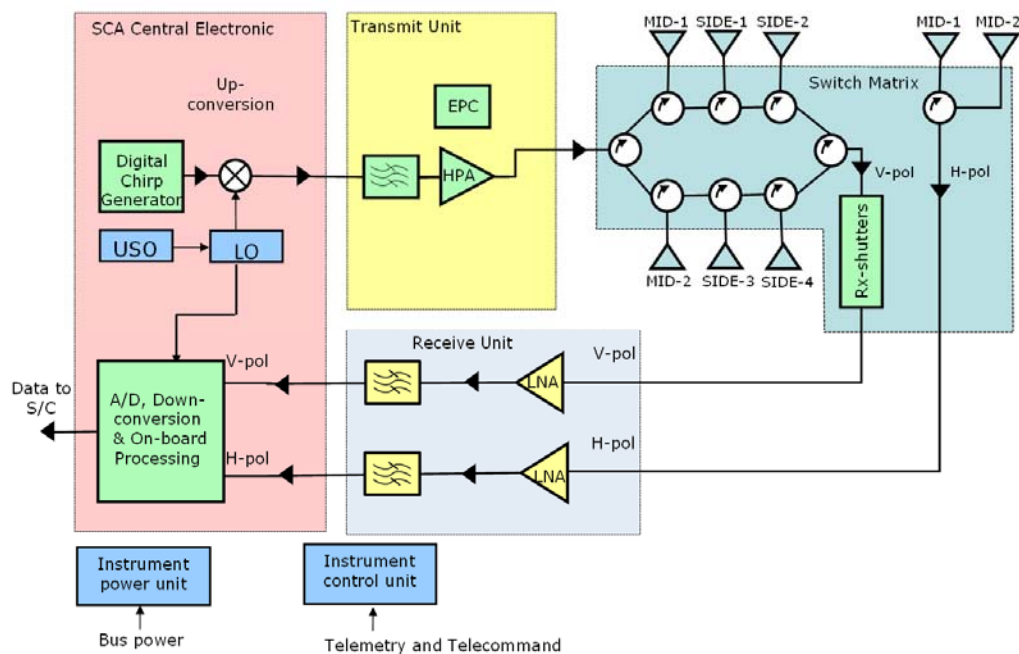


Figure 2: SCA instrument block diagram for the case of simultaneous acquisition of V and H-polarized signals from the mid antennas.

An internal calibration loop measures the transmit pulses at the output of the HPA and that of the beam-switching matrix. The calibration pulses are also injected at the input of the beam-switching matrix and measured at the input of the LNA. Those measurements enable gain characterization of the transmit- and receive-chains, as well as losses of the components in the radar front-end. The necessity of measuring the pulses at the input ports of the antennas is a subject of further analysis in relation to meeting the radiometric stability requirement.

The instrument also measures the thermal noise in the absence of radar echo for determining the background noise level. After the noise estimation on ground, noise subtraction is performed for determining the unbiased ocean surface radar cross-section.

Two possible implementation configurations have been studied for the SCA instrument. These configurations are characterised by the presence of 6 slotted wave guide array antennas. Table 2 summarises the instrument budgets. The ranges correspond to the budgets of the two concepts.

MID Antenna Length	3.20 m
SID Antenna Length	3.55-4.00 m
Average Power	370-430 W
Data Rate	3.2-5.1 Mbit/sec
Mass	420-500 kg

Table 2: SCA instrument budgets

The use of a short, chirp-modulated transmit pulse was assumed for the design optimization. The optimization of the pulse length, taking into account the feasibility of the high power amplifier, has been subject of trade-offs in Phase A.

INSTRUMENT PERFORMANCE

Geophysical Model Function (GMF)

The GMF is an empirically derived function that relates backscatter measurements to surface wind vectors and viewing geometries in the form of $\sigma^0 = \text{GMF}(\text{incidence angle, azimuth angle, wind vector})$. For C-band VV simulations, we use the CMOD5 model for ocean backscatter [1], which is valid for incidence angles ranging from 18 to 58 degrees. For VH simulations, we use an empirical model function derived from the last Radarsat-2 and NOAA SFMR flight campaigns in VH-pol over Hurricanes [3]-[4]. These campaigns confirm a linear tendency of σ^0_{VH} with the wind-speed (as depicted in Figure 3) and a low sensitivity to both incidence and azimuth angles.

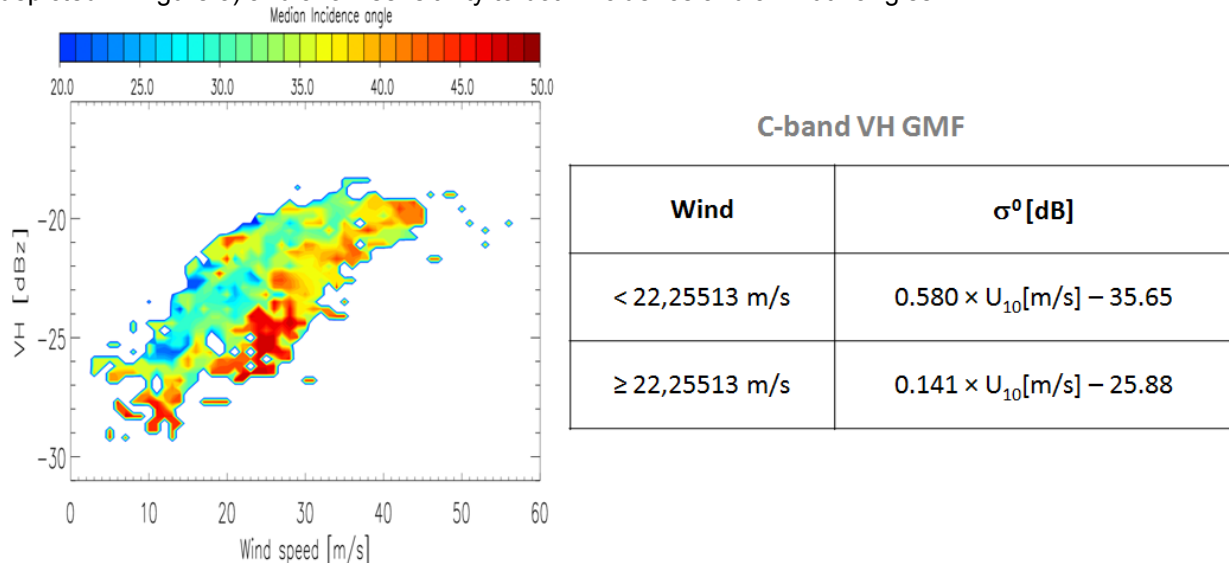


Figure 3: Radarsat-2 versus NOAA SFMR (left); VH-pol Geophysical Model Function (right)

SNR and Radiometric Resolution

The assumptions on backscattering properties (GMF) and nominal atmospheric attenuation affect the expectable echo signal power for a given radar system. For high incidence angles and low cross wind, where the SNR is driving the radiometric resolution performance, about 1.6 dB lower SNR results when applying MetOp-SG specification instead of MetOp specification. Consequently, achieving the same radiometric resolution figures under the MetOp-SG specification implies 1.6 dB higher transmission power or equivalent improvement of antenna gain. The radiometric resolution (K_p) is defined as:

$$Kp = \sqrt{\frac{1}{N_{look}} \left(1 + \frac{1}{SNR}\right)^2 + \frac{1}{N_{noise}} \left(\frac{1}{SNR}\right)^2}$$

where SNR is the average single look signal-to-noise ratio, N_{look} is the number of averaged independent looks and N_{noise} is the equivalent number of averaged noise samples. Figure 4 shows the Signal-to-Noise Ratio in VV-polarisation for the MID and SIDE antennas in case of 25 m/s up-wind (red lines) and 4 m/s cross-wind (blue lines). On the right side, instead, the corresponding radiometric resolution performance versus the requirements in VV-polarisation is shown.

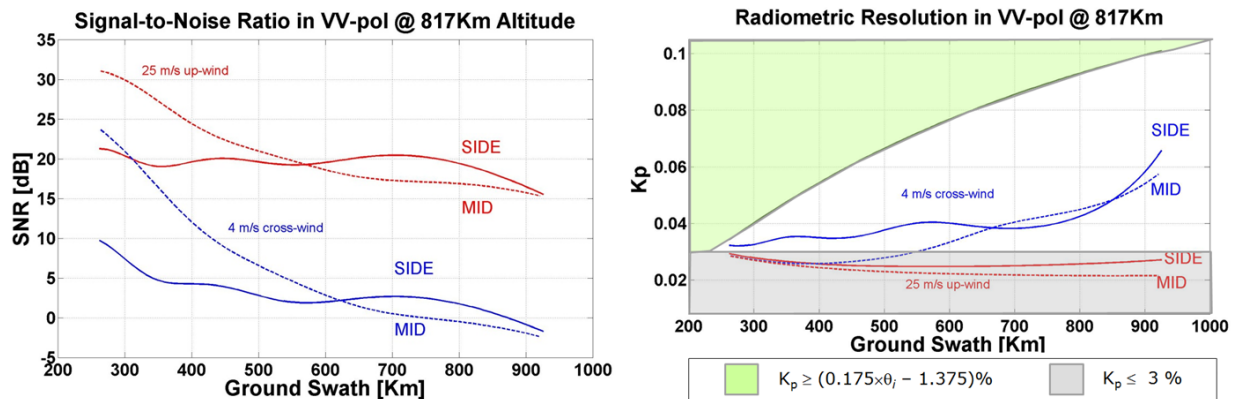


Figure 4: On the left side: Signal-to-Noise Ratio in VV-polarisation for the MID and SIDE antennas in case of 25 m/s up-wind (red lines) and 4 m/s cross-wind (blue lines). On the right side: radiometric resolution performance versus requirements in VV-polarisation.

High Resolution Products

The antenna sizes allow a maximum high resolution product spatial resolution which is approximately given by the FWHM (Full Width at Half Maximum) of a level 1b data product processed such that FWHM is equal in across track and along track direction and the ground filter look efficiency is 1 (i.e. the number of looks collected by the Ground Weighting Function, GWF, is equal to the number of looks which would be collected by a box shaped GWF with box dimensions given by the spatial resolution). The resolution of the high resolution product is shown in Figure 5 (left) together with the predicted radiometric performance (right). The green area in the plot refers to the requirement of the standard-resolution products.

Figure 6 gives an idea of the difference between the instrument Impulse Response Function (IRF) of the standard (left) and high resolution (right) product, for the specific case of SIDE beam in far swath.

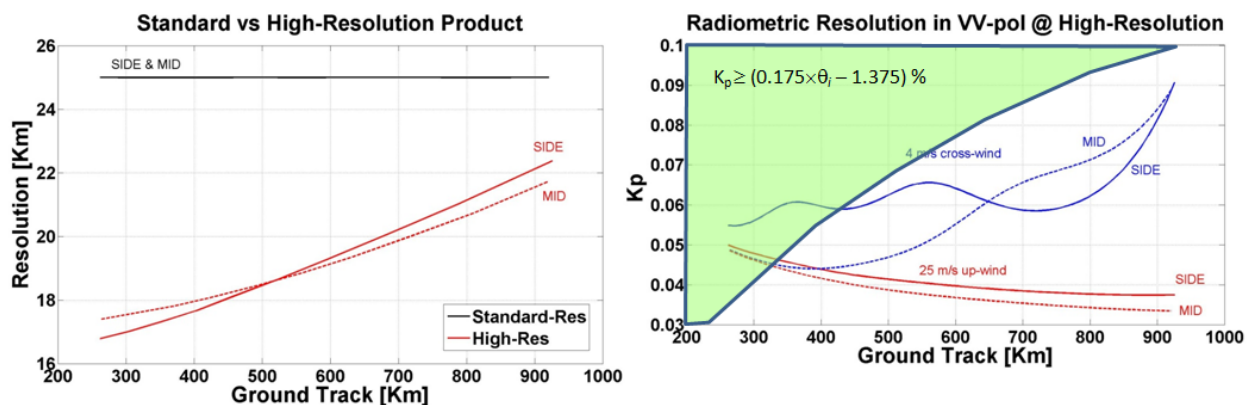


Figure 5: Standard versus high resolution product (left); Radiometric Resolution of the high resolution product in VV-polarisation (right).

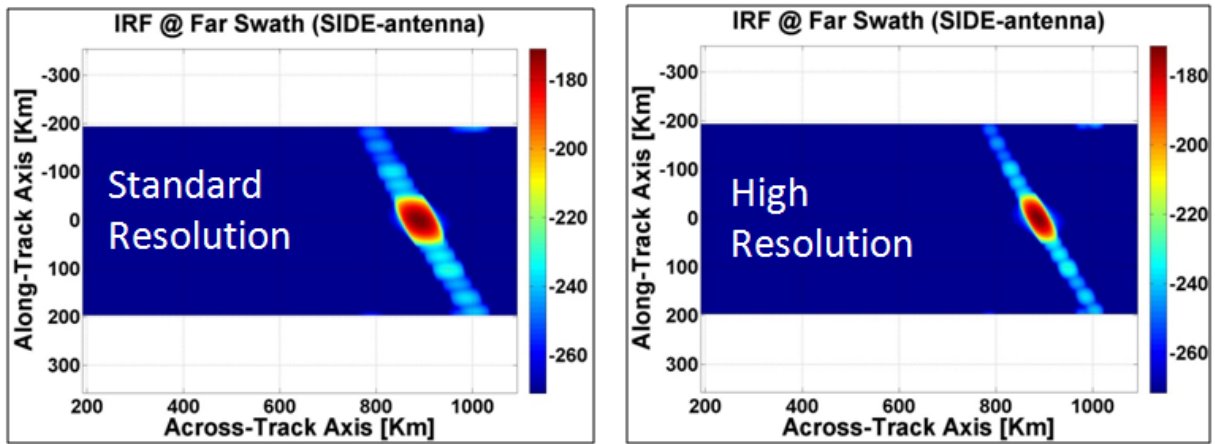


Figure 6: Comparison between the Impulse Response Function of the standard and high-resolution product.

VH data product

The big advantage of the VH-pol with respect to HH-pol and VV-pol is that no apparent saturation of the GMF is visible at high wind speeds (15 m/s ÷ 40 m/s), as depicted in Figure 7 (see also [5]). For the mid beam VH data product, presently, no performance requirement in terms of radiometric resolution is established. It is anyway interesting to compare the radiometric resolution in VH-pol with the VV-pol requirement. To this aim, two extreme cases are investigated in Figure 8; they refer to 15 m/s and 40 m/s wind speed.

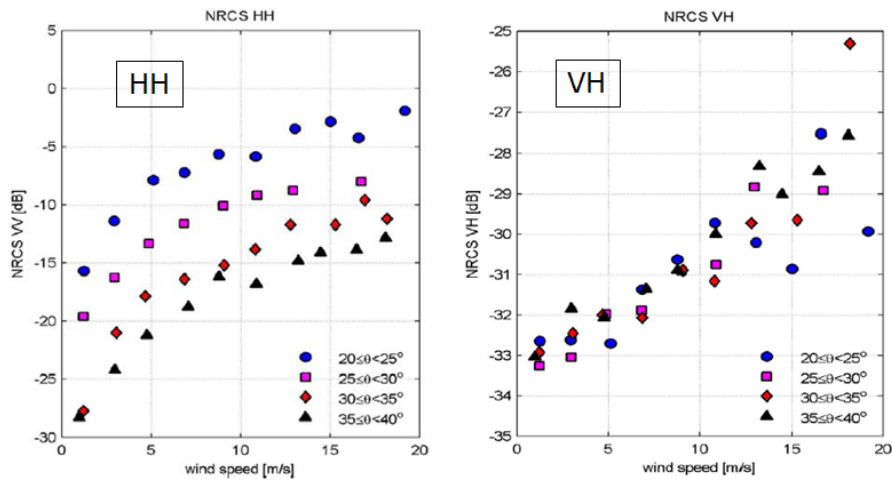


Figure 7: Normalised radar cross section versus wind speed in HH and VH polarisation.

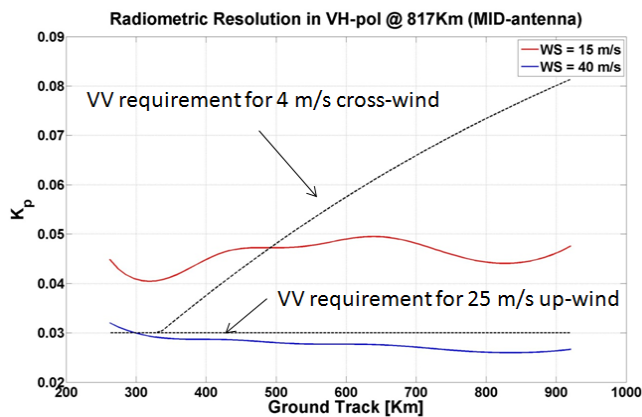


Figure 8: Radiometric resolution in VH-pol for the case of 15 m/s and 40 m/s wind speed.

EXTERNAL CALIBRATION APPROACH

The SCA timing is based on the use of transmission pulses which are much shorter than those of ASCAT (600 μ s against 8.5 ms and 10.8 ms respectively). For sake of clarity, the SCA TX/RX timing is shown in Figure 9. The essential difference is that the transmit pulse length is now shorter than the noise measurement window. Therefore reception of a transponder response can, in principle, be accommodated within the noise measurement window. This window is ideally suited for calibration reception, as it is not contaminated by clutter. If a time delaying transponder is set-up to inject its signal into the noise measurement slot, then a transparent calibration method can be implemented. For the transparent calibration, it is only necessary that the ground processing is aware of the presence of the transponder echoes within the noise window. Since SCA does not use an on-board processing, it is not necessary that the on-board software is aware of the presence of calibration signals. In the ground processor, the noise data packets containing transponder echoes will be separated from the nominal noise data stream and processed separately. The calibration processing is mostly identical to the ASCAT [6] calibration processing, with the exception that signal demodulation and timing has to be adapted to SCA. Transponder echoes are present in the noise window for about 10 s per over flight. This is a small time interval when compared with 150 s noise integration time employed in the nominal ground processing. Therefore, there is no specific need to compensate for the lost noise measurements. With the external calibration being transparent to the space segment, it is possible to continuously acquire calibration data and decide when new sets of calibration data need to be injected into the level 1b processor. Explicit calibration campaigns would no longer be needed. In principle, more than one transponder echo (up to three) could be received at the same time, when the transponders are aligned along the direction of an antenna footprint. As it can be seen from Figure 9, the duration of the noise window can easily be extended without impact on the overall timing concept if a larger margin for timing tolerances is desired.

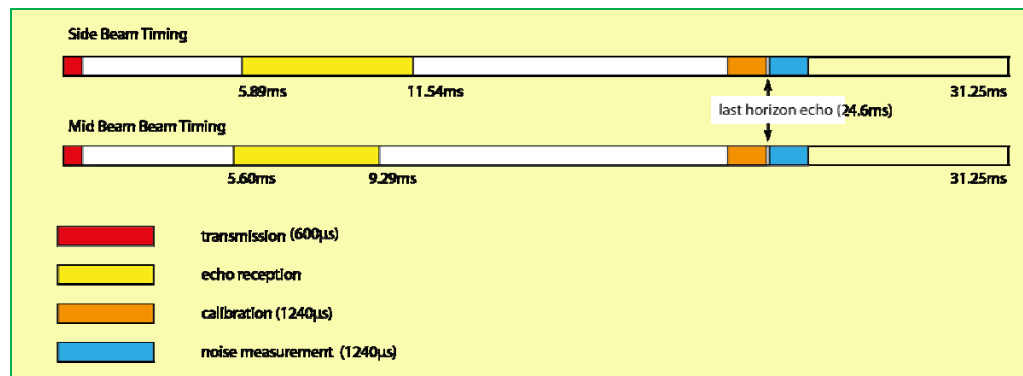


Figure 8: SCA Instrument Timing

REFERENCES

- [1] A. Verhoef, M. Portabella, A. Stoffelen and H. Hersbach, CMOD5.n - the CMOD5 GMF for neutral winds, OSI SAF report, SAF/OSI/CDOP/KNMI/TEC/TN/165, 2008, available at <http://www.knmi.nl/scatterometer/publications/>
- [2] M. Portabella and A. Stoffelen, "Scatterometer Backscatter Uncertainty due to Wind Variability," IEEE Trans. Geosc. & Remote Sensing, Vol. 44, pp. 3356-3362, Nov. 2006.
- [3] G.J. van Zadelhoff, A. Stoffelen, P. Vachon and J. Wolfe, Derivation of a cross-polarization GMF at extreme wind speeds from Radarsat-2 measurements, International Ocean Vector Wind Science Team Workshop, Utrecht, June 2012.
- [4] S. Frasier, J. W. Sapp, P.S. Chang, Z. Jelenak, M. Baker, Airborne Cross-polarization Observations of the sea-surface NRCS in High-Winds, International Ocean Vector Wind Science Team Workshop, Utrecht, June 2012.
- [5] M. Belmonte Rivas, A. Stoffelen, G.J. van Zadelhoff, Polarisation options for ASCAT second generation, International Ocean Vector Wind Science Team Workshop, Utrecht, June 2012.

- [6] J.J.W. Wilson, C. Anderson, M.A. Baker, H. Bonekamp, Radiometric Calibration of the Advanced Wind Scatterometer Radar ASCAT Carried Onboard the METOP-A Satellite, IEEE Transactions on Geoscience and remote Sensing, 2010.